# SeismicAirgun User Guide

Leighton M. Watson
Stanford University
leightonwatson@stanford.edu

February 9, 2020

## I. Introduction

**SeismicAirgun** computes airgun/bubble dynamics following a similar treatment to the seminal work of Ziolkowski (1970). A lumped parameter model is used where the internal properties of the airgun and bubbles are assumed to be spatially uniform. **SeismicAirgun** is written in `MATLAB` and runs efficiently on a standard desktop/laptop computer. For more details and examples of the application of **SeismicAirgun** see:

- Chelminski, S., Watson, L. M., and Ronen, S. (2019) Low-frequency pneumatic seismic sources, *Geophysical Prospecting*, 1-10, https://doi.org/10.1111/1365-2478.12774.
- Watson, L. M., Jennings, J., and Ronen, S. (2017) Source designature of ocean-bottom node data using deterministic airgun modeling, *SEG Technical Program Expanded Abstracts 2017*, 121-126, https://doi.org/10.1190/segam2017-17750879.1.
- Watson, L. M., Dunham, E. M., and Ronen, S. (2016) Numerical modeling of seismic airguns and low-pressure sources, *SEG Technical Program Expanded Abstracts*, 219-224, https://doi.org/10.1190/-segam2016-13846118.1.

## II. Directory

- **source** - function files associated with numerical implementation.
- **doc** - documentation including user guide and license file.
- **references** - publications that are associated with this code.

**SeismicAirgun** is freely available online at https://github.com/leighton-watson/SeismicAirgun and is distributed under the MIT license (see `license.txt` for details).

# III. Model Description

Here, I describe the mathematical model of **SeismicAirgun**, which is a lumped parameter model where the internal properties of the airgun and bubble are assumed to be spatially uniform. The model can be divided into three components; i.) bubble, ii.) airgun, and iii.) acoustic radiation. For more details see Chelminski et al. (2019) and Watson et al. (2016) and the references therein.

## i. Bubble

The motion of the bubble wall is governed by the modified Herring equation (Herring, 1941; Cole, 1948; Vokurka, 1986):

$$R\ddot{R} + \frac{3}{2}\dot{R}^2 = \frac{p_b - p_\infty}{\rho_\infty} + \frac{R}{\rho_\infty c_\infty}\dot{p}_b - \alpha\dot{R}, \tag{1}$$

where $R$, $\dot{R} = dR/dt$, and $\ddot{R} = d^2R/dt^2$ are the radius, velocity, and acceleration of the bubble wall, respectively, $p_b$ is the pressure inside the bubble, $\dot{p}_b = dp_b/dt$, and $p_\infty, \rho_\infty$ and $c_\infty$ are the pressure, density, and speed of sound, respectively, in the water infinitely far from the bubble. The ambient pressure at the depth of the airgun, $z$, is given by $p_\infty = p_{\text{atm}} = \rho_\infty g z$, where $p_{\text{atm}}$ is the atmospheric pressure and $g$ is the gravitational acceleration. Mechanical energy dissipation mechanisms, which are challenging to model directly, are parameterized into an extra damping term of the form of $\alpha\dot{R}$, where $\alpha$ is an empirically determined constant Langhammer and Landrø (1996); Watson et al. (2017).

The bubble is initialized with a finite initial volume equal to the volume of the airgun. This is because the modified Herring equation (equation 1) becomes singular when $R \to 0$. The bubble wall velocity is initially zero and the bubble air is at the same temperature and pressure as the ambient water. The mass can then be calculated from equation 8. For more discussion on the bubble initial conditions see Watson et al. (2019).

Mass is ejected from the airgun into the water forming a bubble if three conditions are met:

1. $t < t_{\text{fire}}$. This parameter can be used to imposed a finite discharge duration.
2. $p_a(t) > p_b(t)$. The airgun only discharges if the pressure inside the source is larger than the pressure outside.
3. $m_a(t) > F\ m_{a0}$ where $m_a(t)$ is the mass in the airgun, $F \in [0, 1]$ is a tunable parameter that controls the fraction of mass ejected from the airgun, and $m_{a0}$ is the initial mass in the airgun.

Mass flow from the airgun to the bubble is given by:

$$\frac{dm_b}{dt} = \begin{cases} p_a A \left(\frac{\gamma}{QT_a}\right)^{1/2} \left(\frac{2}{\gamma-1}\right)^{1/2} \left[\left(\frac{p_a}{p_b}\right)^{(\gamma-1)/\gamma} - 1\right] & \text{if flow is unchoked} \\ p_a A \left(\frac{\gamma}{QT_a}\right)^{1/2} & \text{if flow is choked} \end{cases} \tag{2}$$

where $m_b$ is the mass of the bubble, $A$ is the airgun port area, $Q$ is the specific gas constant, and $p_a$ and $T_a$ are the airgun pressure and temperature, respectively. Flow through the port is choked (choked flow is when the flow through a nozzle has a velocity equal to the sound speed, the maximum possible velocity for fluid flow through a nozzle) if (Babu, 2014)

$$\frac{p_a}{p_b} \geq \left(\frac{\gamma+1}{2}\right)^{\gamma/(\gamma-1)}, \tag{3}$$

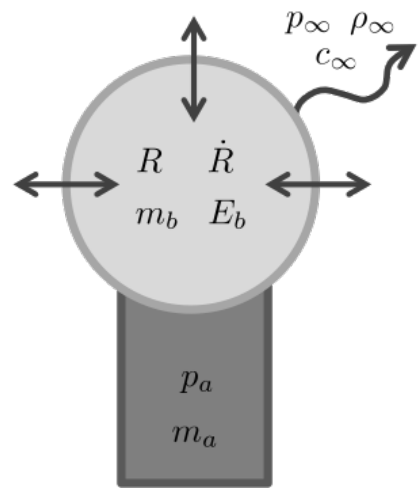


**Figure 1:** *Model schematic. The airgun and bubble are treated as lumped parameter objects. The internal properties are assumed to be spatially uniform and described by a single value that evolves in time.*

where $\gamma$ is the ratio of heat capacities. If the pressure ratio is less than this critical value then flow through the port will be unchoked.

The internal energy of the bubble, $E_b$, changes according to the first law of thermodynamics for an open system:

$$\frac{dE_b}{dt} = c_p T_a \frac{dm_b}{dt} - 4\pi M \kappa R^2 (T_b - T_\infty) - p_b \frac{dV_b}{dt}, \tag{4}$$

where $c_p$ is the heat capacity at constant volume, $\kappa$ is the heat transfer coefficient, $M$ is a constant that accounts for the increased effective surface area over which heat transfer can occur as a result of turbulence at the bubble walls (Laws et al., 1990), and $V_b = (4/3)\pi R^3$ is the volume of the bubble, which is assumed to be spherical.

The bubble of air is less dense than the surrounding water and hence moves buoyantly upwards in the water column. The vertical velocity of the bubble is given by Herring (1941); Taylor (1942); Langhammer and Landrø (1996)

$$\frac{dz(t)}{dt} = \frac{-2g\beta}{R(t)^3} \int_0^t R(\tau)^3 \, d\tau, \tag{5}$$

where $\beta$ is a tunable parameter. As the bubble moves vertically upwards the pressure in the water, $p_\infty$, decreases which results in the bubble oscillating slower.

## ii. Airgun

The airgun and bubble are coupled by conservation of mass:

$$\frac{dm_a}{dt} = -\frac{dm_b}{dt}, \tag{6}$$

where $m_a$ is the mass of air inside the airgun, and conservation of energy:

$$\frac{dE_a}{dt} = -c_p T_a \frac{dm_b}{dt}, \tag{7}$$

where $E_a$ is the internal energy of the airgun.

The airgun and bubble governing equations are closed with the ideal gas equation of state:

$$p = \frac{mQT}{V}, \tag{8}$$

and the relationship between the internal energy and temperature:

$$E = c_v m T, \tag{9}$$

where $c_v$ is the heat capacity at constant volume.

## iii. Acoustic Radiation

The pressure perturbation in the water is related to the bubble dynamics by (Keller and Kolodner, 1956)

$$\Delta p(r,t) = \rho_\infty \left[ \frac{\ddot{V}(t - r/c_\infty)}{4\pi r} - \frac{\dot{V}(t - r/c_\infty)^2}{32\pi^2 r^4} \right], \tag{10}$$

where $\Delta p$ is the pressure perturbation in the water, $r$ is the distance from the center of the bubble to the receiver, and $V$ is the volume of the bubble. The second term on the right side is a near-field term that decays rapidly with distance. In addition to the direct arrival there is a ghost arrival, which is the initially upgoing wave that is reflected with negative polarity from the sea surface. For a receiver directly below the source the observed pressure perturbation is

$$\Delta p_{\text{obs}}(r,t) = \Delta p_D(r,t) - \Delta p_G(r + 2D, t), \tag{11}$$

where $\Delta p_D$ is the direct signal and $\Delta p_G$ is the ghost arrival, which is assumed to have -1 reflection coefficient from the sea surface. $D$ is the depth of the seismic airgun (Figure 2).

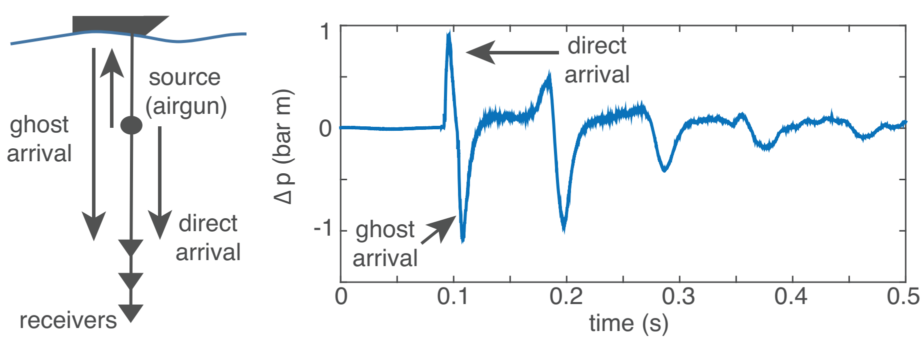


**Figure 2:** *Schematic showing direct and ghost arrivals along with example source signature from Watson et al. (2016).*

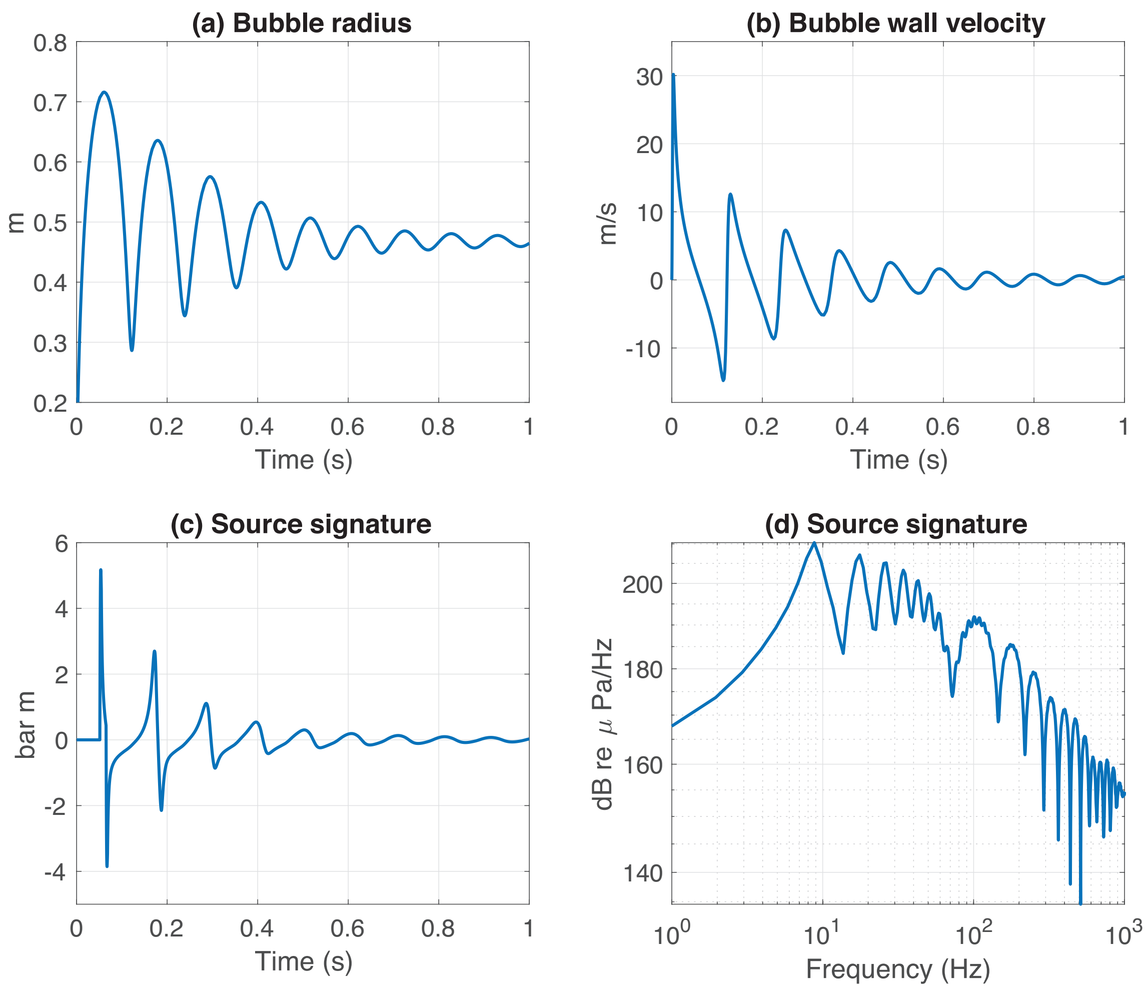


**Figure 3:** *Example model outputs for a 1000 in$^3$ airgun pressurized to 1600 psi with a port area of 16 in$^2$ fired at a depth of 10 m showing (a) bubble radius, (b) bubble wall velocity, and source signature (acoustic pressure perturbation in the water) in the (c) time and (d) frequency domains. The source signature in the time domain is displayed in bar m, which enables comparison between observations at different source-receiver distances.*

## IV. Numerical Implementation

**SeismicAirgun** solves a system of eight ordinary differential equations using `MATLAB`'s built-in solver, `ode45`, which is explicit Runge-Kutta (4,5) method. The variables that are evolved are (1) $R$, bubble radius, (2) $\dot{R}$, bubble wall velocity, (3) $m_b$, the mass of bubble, (4) $T_b$, temperature of bubble, (5) $p_a$, pressure inside the airgun, (6) $m_a$, mass of air inside the airgun, (7) $z$, depth of the bubble, and (8) the integrand in equation 5.

## V. Tuning Parameters

In addition to the source pressure, volume, depth and port area, there are three tuning parameters. Each parameter controls a different part of the source signature:

- $\alpha$: parameterization of additional damping terms. Controls amplitude decay of signature.
- $\beta$: controls the rate of ascent of the bubble. Influences the ambient pressure, $p_\infty$, and hence the bubble period. $\beta$ is especially important for the later bubble oscillations.
- $F$: controls how much mass is ejected from the source. Influences the mass of bubble and hence bubble period. $F$ is especially important for the initial bubble oscillations.

Figure 4 shows the influence of the tuning parameters on the source signature. Increasing $\alpha$ results in more a more rapidly damped source signature (Figure 4a). Increasing $F$ means that less mass is ejected from the source. This results in a smaller bubble that oscillates faster (Figure 4b). Increasing $\beta$ results in the bubble rising faster. This decreases the ambient pressure and causes the bubble to oscillate slower (Figure 4c).

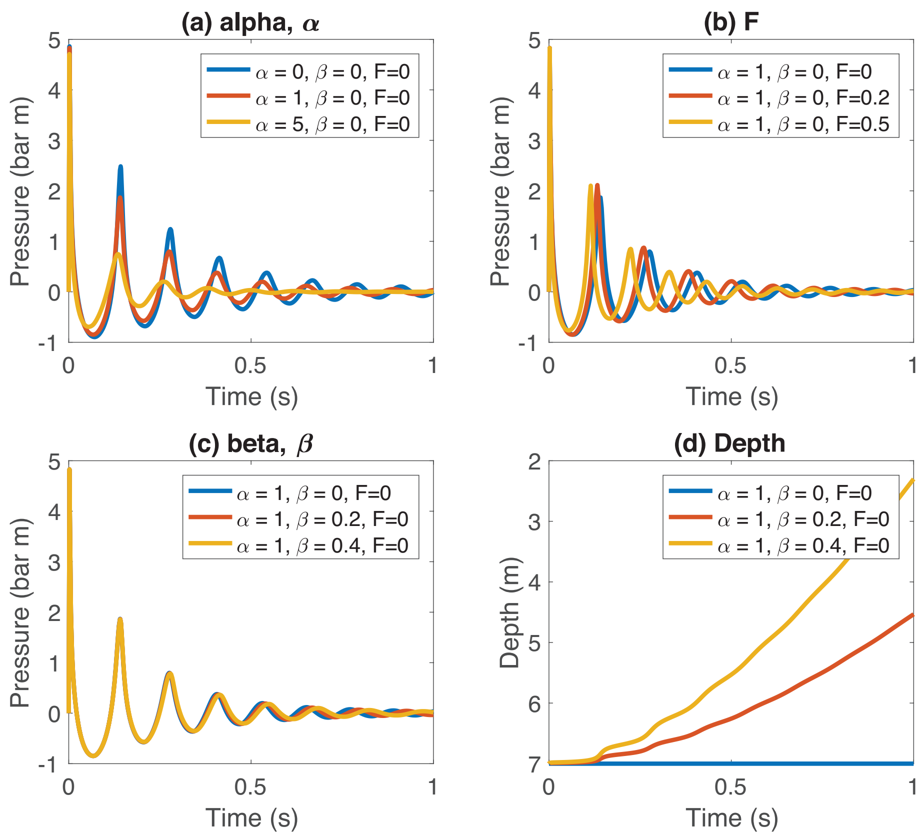


**Figure 4:** *Influence of tuning parameters on the simulated source signature for a 400 in$^2$ source at pressure of 2000 psi, port area of 10 in$^2$ and a depth of 7 m. (a) Varying damping parameter $\alpha$. (b) Varying fraction of mass ejected from source, $F$. (c) Varying ascent rate of bubble, $\beta$. (d) Depth of bubble as a function of time associated with signatures shown in (c).*

# VI. Using SeismicAirgun

Several example script files are include that demonstrate how to specific source properties, run the code, save and display the outputs, and compare the simulation results to *Nucleus* signatures. The three example script files provided are:

- `example_main.m`: shows how to specify source properties, run the code, display basic outputs, and save the simulation result.
- `example_dispOutputs.m`: demonstrates how to plot other outputs from the simulation.
- `example_compareNucleus.m`: compares the simulation results with *Nucleus* data (contained in `nuc.csv` and `nucProperties.csv`).

## i. `example_main.m`

The source contained is contained in the directory `source`. Therefore, the first thing to do is to point to this directory:

```
addpath source/
```

The source firing properties are specified:

```
% Source Firing Configuration
src_pressure = 1000; % source pressure [psi]
src_volume = 10000; % source volume [in^3]
src_area = 80; % port area of source [in^2]
src_depth = 10; % depth of source [m]
% pressure (psi), volume (in^3), port/throat area (in^2)
src_props = [src_pressure, src_volume, src_area];
```

Logical flags are used to determine if the user wants to direct arrival (no ghost) to be plotted (in time and frequency domains) and saved (in ascii and binary formats).

```
% save direct arrival
save_outputs = false; % false = do not save outputs, true = save outputs
% plot direct arrival
plot_outputs = false; % false = do not plot outputs, true = plot outputs
```

There are several physical (distance from source to receiver, total simulation time, sampling interval) and tuning parameters ($\alpha$ in equation 1 and $\beta$ in equation 5) that need to be specified. Parameters are saved to the structure `physConst` using the function file physical_constants. The mass fraction ejected from the airgun, $F$, is directly specified in physical_constants.

```
% Physical and Tuning Parameters
r = 100; % distance from source to receiver.
time = [0 2]; % time [s]
dt = 1.25e-5; % sampling interval
% tuning parameters
alpha = 0.8; % decay of amplitude of pressure perturbation
beta = 0.45; % rate of ascent of bubble
F = 0.4; % fraction of mass that is not ejected from source
physConst = physical_constants(src_depth, r, time, alpha, beta, F); % physical constant
```

The solver is run by calling `SeismicAirgun`:

```
output = SeismicAirgun(src_props, physConst, dt, plot_outputs);
```

Outputs can be saved in a variety of formats: ascii, binary and (work in progress) SEGY.

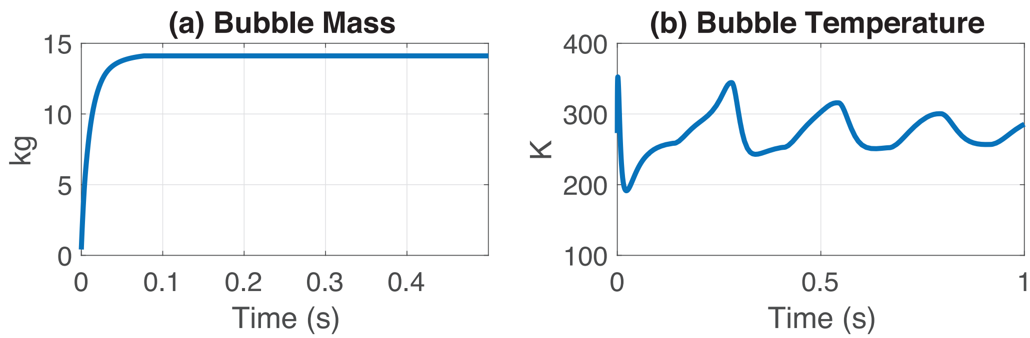


**Figure 5:** *Example model outputs for a 10,000 in$^3$ airgun pressurized to 1000 psi with a port area of 80 in$^2$ fired at a depth of 10 m showing (a) bubble mass and (b) temperature.*

### ii. `example_dispOutputs.m`

This script file is very similar to `example_main.m` with the addition of demonstrating how to plot additional outputs, such as mass and temperature of the bubble (Figure 5).

### iii. `example_compareNucleus.m`

*Nucleus* is a commercial airgun modeling software produced by PGS. The **SeismicAirgun** git repository contains 65 example *Nucleus* signatures (containing just the direct arrival). The source properties (pressure and volume) are contained in `nucProperties.csv` while the time series data is contained in `nuc.csv`.

`example_compareNucleus.m` compares the simulated signatures using **SeismicAirgun** with the *Nucleus* signatures. A similar comparison is presented in Watson et al. (2017). The source pressure and volume are selected to match the *Nucleus* values:

```
src_pressure = nucProp(i,1); % source pressure [psi]
```

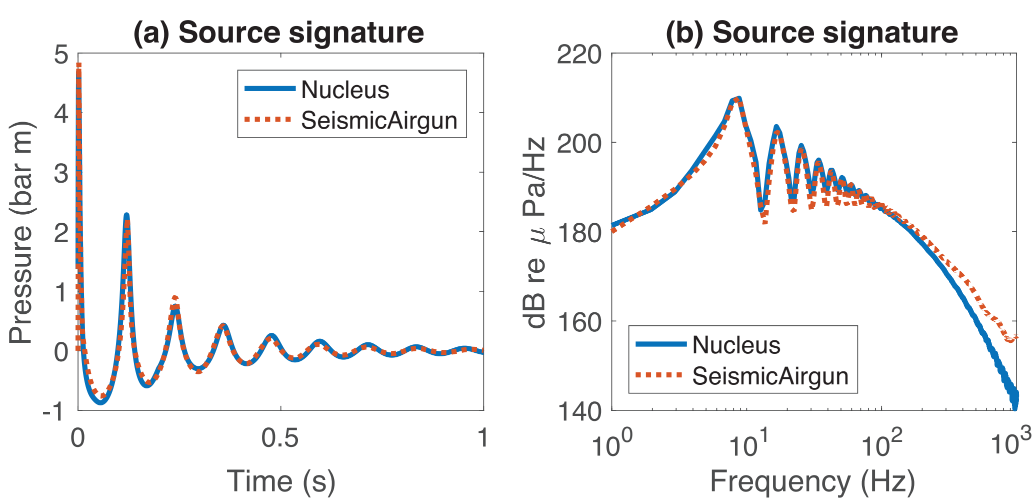


**Figure 6:** *Example model outputs for a 400 in$^3$ airgun pressurized to 2000 psi. Source depth is 7 m and port area is assumed to be 10 in$^2$. Tuning parameters are $\alpha = 0.8$, $\beta = 0.45$ and $F = 0.4$.*

```
src_volume = nucProp(i,2); % source volume [in^3]
```

The other parameter values are the port area, source depth, and the tuning parameters $\alpha$, $\beta$, and $F$. **SeismicAirgun** is able to provide a good match to *Nucleus*, as shown in Figure 6.

Note that **SeismicAirgun** is limited to a single source and cannot rigorously account for the complex interactions between bubbles generated by multiple sources in close proximity.

## References

Babu, V., 2014. Fundamentals of Gas Dynamics, 2nd Edition. John Wiley & Sons, Chichester.

Chelminski, S., Watson, L. M., Ronen, S., 2019. Low frequency pneumatic seismic sources. Geophysical Prospecting, 1–10.

Cole, R. H., 1948. Underwater explosions. Princeton University Press, Princeton.

Herring, C., 1941. Theory of the pulsations of the gas bubble produced by an underwater explosions. Tech. rep., Office of Scientific Research and Development.

Keller, J. B., Kolodner, I. I., 1956. Damping of underwater explosion bubble oscillations. Journal of Applied Physics 27 (10), 1152–1161.

Langhammer, J., Landrø, M., 1996. High-speed photography of the bubble generated by an airgun. Geophysical Prospecting (44), 153–173.

Laws, R. M., Hatton, L., Haartsen, M., 1990. Computer modelling of clustered airguns. First Break 8 (9), 331–338.

Taylor, G. I., 1942. The vertical motion of a spherical bubble and the pressure surrounding it. Tech. rep., Office of Naval Research, Dept. of the Navy.

Vokurka, K., 1986. Comparison of Rayleigh's , Herring's , and Gilmore's Models of Gas Bubbles. Acta Acustica united with Acustica 59 (3), 214–219(6).

Watson, L. M., Dunham, E. M., Ronen, S., 2016. Numerical modeling of seismic airguns and low-pressure sources. In: SEG Technical Program Expanded Abstracts 2016. No. 1. pp. 219–224.

Watson, L. M., Jennings, J., Ronen, S., 2017. Source designature of ocean bottom node data using deterministic airgun modeling. SEG Technical Program Expanded Abstracts 2017, 121–126.

Watson, L. M., Werpers, J., Dunham, E. M., 2019. What controls the initial peak of an air gun source signature? Geophysics 84 (2), P27–P45.

Ziolkowski, A., 1970. A Method for Calculating the Output Pressure Waveform from an Air Gun. Geophysical Journal International 21 (2), 137–161.